INTRACELLULAR DELIVERY OF CRISPR-CAS9 VIA A SYNTHESIZED LIPID-LIKE NANOPARTICLE LIBRARY FOR GENE EDITING

By

Justin Bolinger

A Thesis Submitted in Partial Fulfillment

of the Requirements for the Degree of

Master of Science

In

Biomedical Engineering

Department of Biomedical Engineering
Tufts University
Medford, MA
May 2018

Thesis Defense Committee:

Qiaobing Xu, Associate Professor, Department of Biomedical Engineering, Principal Investigator
Sergio Fantini, Professor, Department of Biomedical Engineering
James Van Deventer, Assistant Professor, Chemical and Biological Engineering

ABSTRACT

The field of protein therapeutics is an emerging one. One of the evident challenges of protein therapeutics is the method of delivering these proteins, which are often fragile or prone to break down. Lipid nanoparticles (LNPs) represent a class of drug delivery system that has shown promise for providing an efficient vehicle for protein therapeutics.

The hypothesis of this study was that fabricated LNPs could carry out CRISPR deliveries of model proteins at transfection efficiencies comparable to a commercially available lipid. 20 LNPs were synthesized using a self-assembly fabrication method to create a congener library. The LNPs comprising this library were confirmed structurally and their physical stability profiles were determined. GFP-Cre was delivered to HeLa-DsRed cells via these LNPs to determine their ability to enable protein uptake by assessing induced GFP fluorescence. Similarly, Cas9:sgRNA complexes targeting GFP were delivered to GFP-HEK cells to assess their GFP knockout efficiencies by assessing GFP fluorescence.

20 formulated and 20 non-formulated LNPs were produced. Transmission electron microscopy and dynamic light scattering analysis were used to confirm that the fabricated LNPs had uniform size and shape as well as uniform stability profiles and relatively homogenous particle size. For the delivery of GFP-Cre with the 20 formulated LNPs, 12 were able to induce GFP fluorescence at a rate of greater than 30%, with 10 performing similar to or better than the positive control, Lipofectamine 2000 (~45% GFP-positive). For the delivery of

Cas9:sgRNA with the 20 formulated LNPs, 13 were able to induce GFP knockout at a rate of greater than 30%, with 6 performing similar to or better than the positive control (~65%). MTT assay data showed 6 formulated LNPs which yielded high values for cell viability (greater than 90%). A combination of these data gave us 5 formulated LNPs with high transfection efficiencies and low cytotoxicities, making these LNPs attractive for further research.

ACKNOWLEDGMENTS

I would first like to acknowledge my principal investigator, Dr. Qiaobing Xu, who has helped guide my research for the last two years. From the first day we met to discuss initial project ideas, you have been there to work with my scattered thoughts and crazy work schedule to achieve great work in your lab. The reason I spent all those nights running samples well past 3 am is because I believe in advancing the lab's goals to investigate lipid nanoparticles from all angles. Thank you for advising my research in an exciting, meaningful direction.

Thank you to everyone in the Xu lab. Your support and friendships mean the world to me. Know that I tried every day to leave the lab a better place than when I came in. I wish you all the best of luck in your ongoing experiments and future endeavors.

Thank you to Milva Ricci for always being willing to approve my requests for access to lab after lab, as well as for our discussions about life and football.

Perhaps most deserving of recognition is my research mentor, Dr. Yamin Li. You diligently taught me how to perform success CRISPR-Cas9 deliveries and countless other laboratory techniques to the point where I feel comfortable training others. I've always looked up to the dedication you have for your craft as a scientist, and your words of encouragement, criticism, and wit will always stick with me. Words cannot express my gratitude for your patience, continuing support, and friendship.

TABLE OF CONTENTS

Section **Page**

FIGURES

Figure **Page**

TABLES

Table **Page**

1. Introduction

The delivery of therapeutic proteins is an ever-expanding field with numerous applications like mediation of cell function and genome-editing. Proteins like Cas9 have recently been shown to be effective in altering targeted segments of DNA, a process which has reinvigorated the field of protein-based therapeutics for treatments of genetic diseases and cancers alike. Proteins, however, can be inherently unstable, especially those formulated for these types of treatments. Therefore, one of the biggest challenges of delivering protein therapeutics is the unpredictable nature of the breakdown of these proteins [1]. Naturally derived nanoparticles represent an interesting class of drug delivery system that has shown promise across numerous iterations [2]. If lipid nanoparticles were to show effectiveness at delivering proteins to a targeted location within a cell while maintaining structural and functional integrity of the protein, it would open the door for many new types of genome-targeting therapeutics. Our lab previously demonstrated the effectiveness of delivering of genome-editing proteins using bioreducible lipid nanoparticles [3].

A primary goal of this line of research is to find a better lipid for delivering protein-based therapies or cytotoxic therapies for cancer treatment. This newly discovered lipid can be better than existing methods in a variety of ways. Higher stability is typically desirable because a manufactured lipid product would be more robust and have a commercial shelf-life potentially longer than

existing treatments. Lower cytotoxicity is desirable in cases where the cell targeted by the therapeutic is intended to stay alive, as a lipid nanoparticle that is very cytotoxic will render any changes to the cell not intended to trigger cell death irrelevant. It may be desirable for a lipid nanoparticle to be highly bioavailable, as this could potentially increase the chance of the action desired by the treatment to happen. Perhaps most important is for a lipid nanoparticle to have high delivery efficiency, as this will often be the key metric used to determine the candidacy of a lipidoid to be used in treatments. Therefore, when trying to find better lipids for the delivery of genome-editing therapeutics, it is of interest to consider all of these metrics and determine the best combination of relevant factors that make a lipidoid a strong candidate for further research.

2. Background

To introduce the topics covered in this paper, it is necessary to briefly cover the state of protein therapeutics, the premise behind CRISPR-Cas9, and the nature of lipid nanoparticles. Previously completed work pertaining to this study will also be addressed.

2.1. Protein Therapeutics

The field of protein therapeutics is a relatively young one, with most advancements in the field coming in the last four decades. The approval of recombinant human insulin in 1982 as the first recombinant protein therapeutic marked a turning point for biomedical treatments, as this opened the door for other protein-based therapies to follow in its promising path [4]. Protein therapeutics can be classified into separate categories based on their pharmacological activities: some aid existing biochemical pathways, others provide innovative functions or transport other compounds, while others replace irregular proteins entirely [5]. As of 10 years ago, the US Food and Drug Administration has approved over 130 proteins and peptides [6].

As direct competitors to protein-based therapies, therapies utilizing small-molecule drugs try to target similar problems that both treatments look to address. Small-molecule drugs have been developed to treat a variety of diseases, with pediatric leukemia and psoriasis as recent examples [7][8]. There are many factors

that promote the use of protein therapeutics over small-molecule drugs in some cases. Proteins can be fabricated with more intricate structures and carry out more complicated objectives than small-molecule compounds may be capable of. This specificity of function may help ensure that biological processes not targeted by the protein treatment remain unaffected. In addition, proteins used for therapeutics are often found to naturally occur in the body, diminishing the chance of a detrimental immune response and thereby increasing the biocompatibility of the treatment [6]. Furthermore, studies have shown that protein therapeutics may travel through the tedious processes of clinical development and FDA approval quicker than their small-molecule drug counterparts [9].

2.2. CRISPR-Cas9

CRISPR-Cas9 systems represent a breakthrough in the field of genome editing technology. CRISPR stands for Clustered Regularly Interspaced Short Palindromic Repeats. In bacteria, these repeats are a group of DNA sequences that contain DNA from viruses that have attacked the cell, enabling these microorganisms to possess defense systems
that can more easily recognize and guard against plasmids and viruses by providing the bacteria with adaptive immunity [10]. The CRISPR-Cas9 system was derived from these CRISPR systems found in bacteria.

Cas9 is a CRISPR-associated endonuclease that can cut two strands of DNA at a specific location in a genome [11]. The CRISPR-Cas9 system is

comprised of two parts: the Cas9 enzyme and the guide RNA (gRNA). This gRNA is a pre-determined RNA sequence, usually ~20 base pairs in length, found within a larger RNA scaffold and can be fabricated to locate and bind to a specific DNA sequence. [11] In short, CRISPR-Cas9 works as follows: the gRNA binds to a targeted sequence on one strand of DNA, the Cas9 enzyme binds to the gRNA and cuts both strands of DNA, and the cut is fixed by introducing a predetermined mutation into both strands of DNA. [10][11]

Highlighting a few pros of CRISPR-Cas9, this gene editing system is straightforward, flexible, and specific. CRISPR-Cas9 is only a two-component system, making it relatively easy and convenient to use. The inherent flexibility of CRISPR-Cas9 allows the user to target any known sequence of DNA. The nature of the system also allows the user to focus on precise targets, minimizing chances of error [11].

One of the challenges of CRISPR-Cas9 is facilitating the delivery of the system into the human body so that this treatment can be used across a wide variety of therapeutic applications [12]. This delivery must be carried out in a safe and effective manner, as any benefits of a targeted CRISPR-Cas9 system will be rendered moot if the treatment causes other ailments or is neutralized before reaching its target and performing its desired function. The routes one can take to delivery CRISPR-Cas9 systems are numerous and include electroporation, micro- and hydrodynamic injection, mechanical cell deformation, lenti- and adeno-associated viruses, gold nanoparticles, and lipid and polymer nanoparticles [12]. These methods of delivery all have positive and negative aspects depending on

what the treatment plan, as no one method is a universally sound choice for all CRISPR-Cas9 applications.

Here, we will examine the structure of lipid nanoparticles and their potential as carriers for a CRISPR-Cas9 system.

2.3. Lipid Nanoparticles

Lipid nanoparticles (LNPs) are colloidal dispersions typically made up of lipids, surfactants, and co-surfactants. A variety of lipids may be used including fatty acids and alcohols as well as various glycerides and waxes. To stabilize their dispersions, lipid nanoparticles are often surface-tailored with steroidal or helper lipids. The materials used to manufacturer lipid nanoparticles are usually solid at room temperature. The structure and chemical makeup of a lipid nanoparticle will influence its performance and stability [13].

As a carrier, it is the primary function of a lipid nanoparticle to transport another material, e.g. a drug, to a site and release its cargo at a designated time and place within an organism. These particles are usually designed as sustained-release systems, with the structure of the lipid nanoparticle being the biggest factor in determining the release profile of the therapeutic material [13]. The loading capacity of a lipid nanoparticle is also a critical factor in determining the suitable of such formulations for therapeutic use. For gene therapy, the use of two-tailed cationic lipids may result in improved transfection efficiencies when compared to one-tailed cationic lipids [14].

With respect to their potential use as carriers for CRISPR-Cas9 systems, lipid nanoparticles are safe, biocompatible, and easy to prepare. Lipofectamine 2000, for example, is a commercially available transfection lipid that can be used to transfect different cell lines to edit targeted genes. One of the major drawbacks of lipid nanoparticles is that they typically cannot achieve high delivery efficiencies with respect to transfecting target cells. Another drawback is its high toxicity, making it difficult to use in many applications. Even when taking these limitations into consideration, lipid nanoparticles are usually reasonable options for all CRISPR-Cas9 methodologies [12]. Figure 1 maps out the basic principle behind the delivery of a Cas9:sgRNA/LNP complex to the cell for the purpose of genome editing.

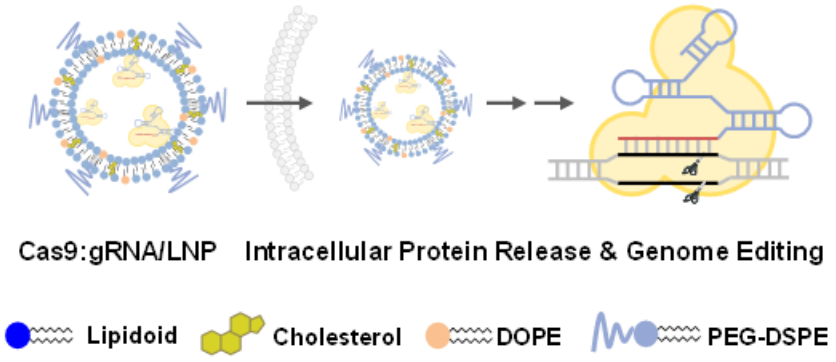

Figure 1. *Intracellular Delivery of Cas9:sgRNA Using Synthetic Lipid Nanoparticles for Genome Editing.*

2.4. Previous Work

Lipid nanoparticles with CRISPR-Cas9 systems have been explored for gene knockout studies in animal models as well as therapeutic treatments [15][16][17].

A previous study in our lab used a combinatorial design strategy to create a library of cationic lipidoids. These lipidoids were shown to serve as an effective platform for protein transport by delivering cytotoxic proteins, ribonuclease A and saporin, into cancer cells and inhibiting their proliferation. This research also showed that to create a stable nanocomplex suitable for protein delivery, electrostatic self-assembly between protein and lipid was critical [18]. Another study showed that these bioreducible lipids, made from the same combinatorial synthesis procedures as above, were able to form nanocomplexes with Cas9:sgRNA ribonucleoprotein (RNP) complexes. These nanocomplexes were able to deliver genome-editing proteins into mouse brain to carry out DNA recombination *in vivo* [3].

3. Objective and Specific Aims

The objective of this study is to expand a library of lipid nanoparticles (henceforth written as LNPs), test these new LNPs across multiple congeners for stability and their ability to deliver CRISPR-Cas9 systems to target cell lines *in vitro*, and assess the lipid nanoparticles from this information for their potential to be used as carriers for protein therapeutics.

The first specific aim of this study is to determine the characteristics and stability profiles of multiple variations of LNPs fabricated by our lab. These chapters will detail how the lipids were initially synthesized as well as how the LNPs were created via self-assembly fabrication methods. These chapters will also assess the LNPs for stability, morphology, and size.

The second specific aim of this study is to determine the efficacies at which these LNPs can deliver different protein complexes to two target cell lines. These chapters will discuss which candidates appear to be the most effective at transfecting their target cells.

The third specific aim of this study to determine the cytotoxicities of these LNPs. These chapters will the results of assays used to assess the LNPs for this property.

The fourth specific aim of this study is to use conclusions drawn from the first three specific aims to evaluate which LNPs represent the best candidates for the delivery of protein therapeutics.

4. Materials

4.1. General

Materials were heated as needed in a water bath (Isotemp® waterbath, Fisher Scientific). Materials were sonicated as needed in a water bath sonicator (Bransonic® Ultrasonic Cleaner Model 5510R-MT, Branson Ultrasonics Corporation). Materials were stirred as needed on stir plates (Thermolyne® Cimarec®, Sigma-Aldrich; VWR Stirrer Model 365, VWR International). Materials were gently agitated as needed by an orbital shaker (DS-500 Orbital Shaker, VWR International). Materials were centrifuged as needed by a centrifuge (GS-6KR Centrifuge, Beckman Coulter Life Sciences).

4.2. Cell Culture

HeLa-DsRed and GFP-HEK cell lines used in this study were obtained from previous experiments in the Xu lab. These cells were thawed from aliquots frozen in liquid nitrogen in the Science and Technology Building at Tufts University, Medford, MA. All cell handling took place in a biosafety cabinet (1300 Series A2 Class II, Thermo Fisher Scientific). Cells were incubated as needed in a CO_2 incubator (Forma Direct Heat CO_2 Incubator, Thermo Fisher Scientific). All incubation steps mentioned occurred at 37 degC and 5% CO_2.

Throughout this paper, ‘cell culture media’ will be used to denote a mixture of Dulbecco’s Modified Eagle’s medium (DMEM), Fetal Bovine Serum

(FBS), and Penicillin-Streptomycin (P-S) at a 100:10:1 volumetric ratio. DMEM, FBS, and P-S were purchased from Sigma-Aldrich. Trypsin used during cell handling was purchased from Sigma-Aldrich.

4.3. LNP Preparation

Amine head groups and lipid components used in the production of the pure lipidoids for the fabrication of LNPs were purchased from Sigma-Aldrich (St. Louis, MO) and Alfa Aesar (Ward Hill, MA). 1,2-Dioleoyl-*sn*-glycero-3-phosphoethanolamine (DOPE), cholesterol, and 1,2-distearoyl-sn-glycero-3-phosphoethanolamine-N-[amino(polyethylene glycol)-2000] (DSPE-PEG(2000)) were used to perform the self-assembly fabrication of the LNPs. DOPE and DSPE-PEG(2000) were purchased from Avanti Polar Lipids (Alabaster, Alabama). Cholesterol was purchased from Sigma-Aldrich. Phosphate buffered saline (PBS) used during LNP preparation and cell handling was purchased from Sigma Aldrich. Nuclease-free water used during LNP preparation and cell handling was purchased from Invitrogen (Carlsbad, CA). Ethanol (100%) and chloroform used during LNP preparation was purchased from Sigma-Aldrich. Sodium acetate used during LNP preparation was purchased from Sigma-Aldrich.

LNPs were subjected to dialysis using 3,500 MWCO (3.5k Da) dialysis cassettes (Slide-A-Lyzer^{TM}, ThermoFisher Scientific).

4.4. CRISPR Deliveries and Cytotoxicity Assay

Cas9 protein used in the CRISPR deliveries was produced by our lab from *E. coli* [3]. Single guide RNA (sgRNA) to insert the GFP gene was produced by the Xu lab using materials from DNA polymerase (Platinum SuperFi Green DNA Polymerase Kit, ThermoFisher Scientific) and RNA synthesis (HiScribe™ T7 High Yield RNA Synthesis Kit, New England BioLabs) kits. GFP-Cre protein was produced by our lab [3]. Lipofectamine 2000 (Lpf2k), used as a commercially available transfection reagent, was purchased from Invitrogen.

3-(4,5-dimethylthiazol-2-yl)-2,5-diphenyltetrazolium bromide (MTT) and dimethyl sulfoxide (DMSO) used during cytotoxicity assays were purchased from Sigma-Aldrich.

4.5. Large Equipment and Associated Software

Flow cytometry was done using fluorescence-activated cell sorting (FACS) equipment (BD FACSCalibur™, BD Biosciences). Data from FACS measurements were collected using BD CellQuest™ Pro software. Data from FACS measurements were analyzed using FlowJo® software.

Hydrodynamic diameters and polydispersity values were measured using dynamic light scattering (DLS) equipment (ZetaPALS Zeta Potential Analyzer, Brookhaven Instruments Corporation). Data from DLS measurements were analyzed using BIC Particle Solutions software.

For MTT assays, absorbance readings were obtained using a microplate reader (SpectraMax M2, Molecular Devices). Microplate reader data was recorded using SoftMax Pro 6 software.

Images of LNPs were taken using transmission electron microscopy (TEM) equipment (Massachusetts Institute of Technology, Cambridge, MA).

5. Methods

To carry out the objective and specific aims of this study, lipidoids will first be synthesized, whereupon they will be further manufactured into LNPs via self-assembly fabrication. Samples of these LNPs will be prepared separately for physical examination and characterization. A CRISPR-Cas9 delivery will take place with two different proteins and cell lines to determine how well these LNPs can facilitate transfection. Last, assays used to determine cytotoxicity will be performed.

5.1. Lipidoid Synthesis and Characterization

5.1.1. Synthesis

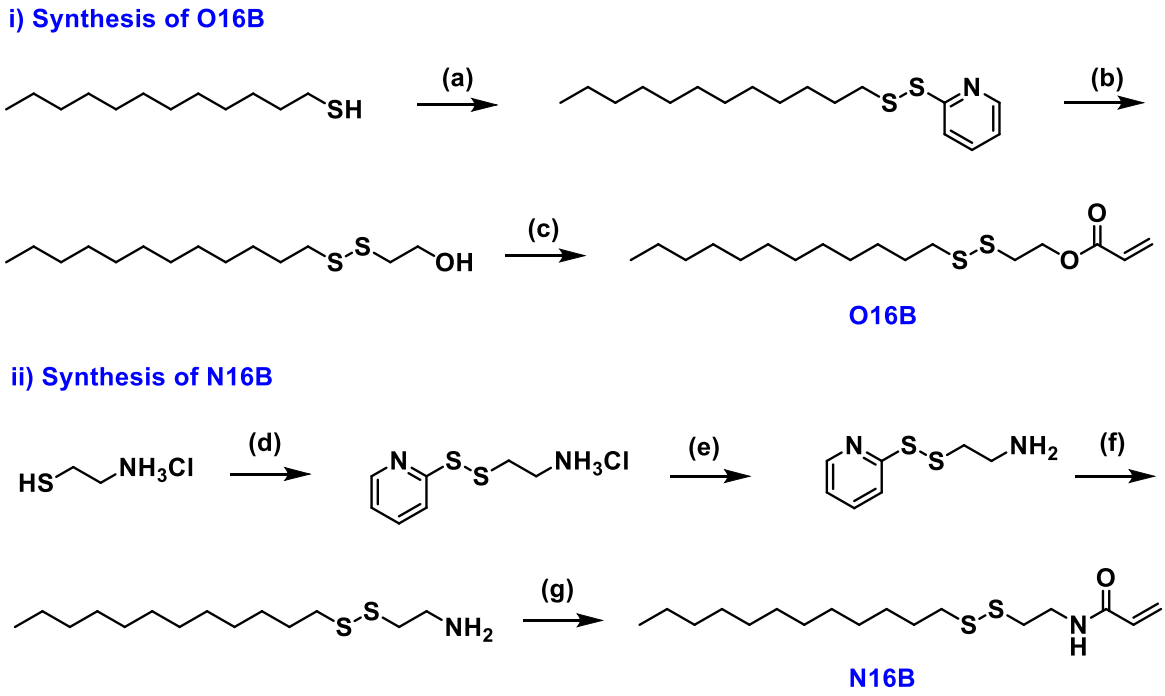

Figure 2. *Synthetic Route Applied for Lipidoid Tails O16B and N16B.* ***(Top)*** *Synthesis of O16B.* ***(Bottom)*** *Synthesis of N16B.*

The pure lipidoids used in this study were created through a series of reactions between amine heads and acrylate tails. First, the lipidoid tails were synthesized using the routes, outlined in Fig. 2, to obtain a hydrophobic acrylate tail of 16 carbons with either an oxygen or nitrogen atom between the acrylate group and disulfide bond. Next, these acrylate tails were reacted with amines to create the final lipidoids used in the fabrication of the LNPs.

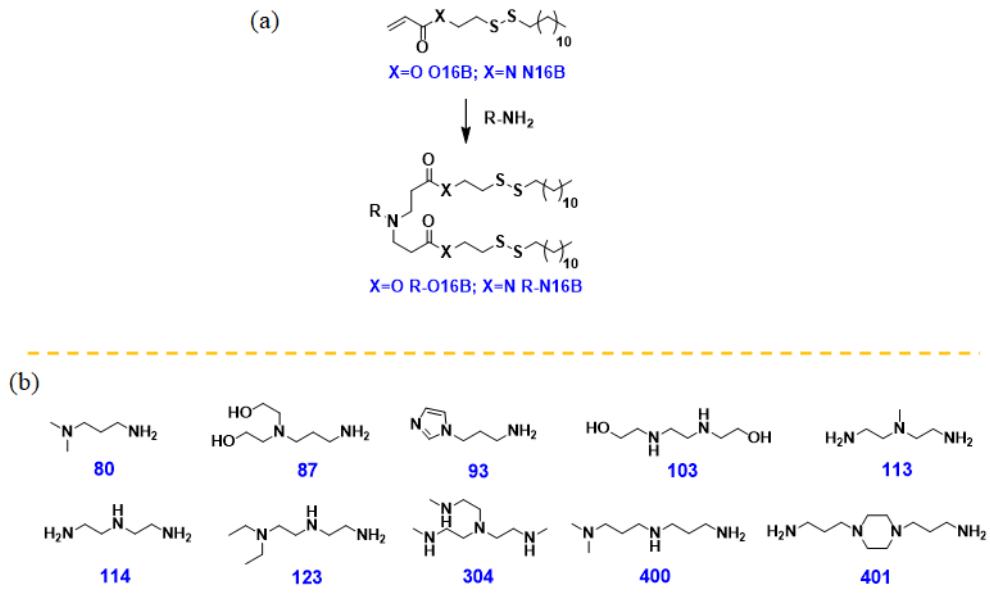

Figure 3. *Technical Components of Lipidoid Synthesis.* ***(a)*** *Simplified Synthesis of Lipid Tail Used for LNP Synthesis.* ***(b)*** *Chemical Structures of Amine Head Groups Used for LNP Synthesis.*

Figure 3a outlines a simplified synthesis of a lipid tail used for synthesis of the LNPs. Figure 3c lists the commercially available amine head groups used in this study. The lipids were named according to the nomenclature of X-Y16B, with X representing the amine number and Y representing the identity of the atom between the acrylate group and the disulfide bond.

List of Pure Lipidoids Used for Fabrication of LNPs	
80-O16B	80-N16B
87-O16B	87-N16B
93-O16B	93-N16B
103-O16B	103-N16B
113-O16B	113-N16B
114-O16B	114-N16B
123-O16B	123-N16B
304-O16B	304-N16B
400-O16B	400-N16B
401-O16B	401-N16B

Table 1. *List of Pure Lipidoids Used for Fabrication of LNPs.* ***(Left)*** *O series LNPs.* ***(Right)*** *N series LNPs.*

20 versions of pure lipidoids were obtained through previously conducted syntheses by the Xu lab (Science and Technology Center, Tufts University, Medford, MA). Table 1 gives a list of the 20 lipidoids used for this study. LNPs found in the left column of Table 1 are O series, while LNPs found in the right column are N series; LNPs on the same row of Table 1 have the same amine head group and differ by only one atom in their lipid tail groups.

5.1.2. NMR Characterization

Figure 4 depicts the ^{1}H and ^{13}C NMR spectra for the O16B tails, while Figure 5 depicts the ^{1}H and ^{13}C NMR spectra for the N16B tails. These measurements were used to confirm the structures of these tails.

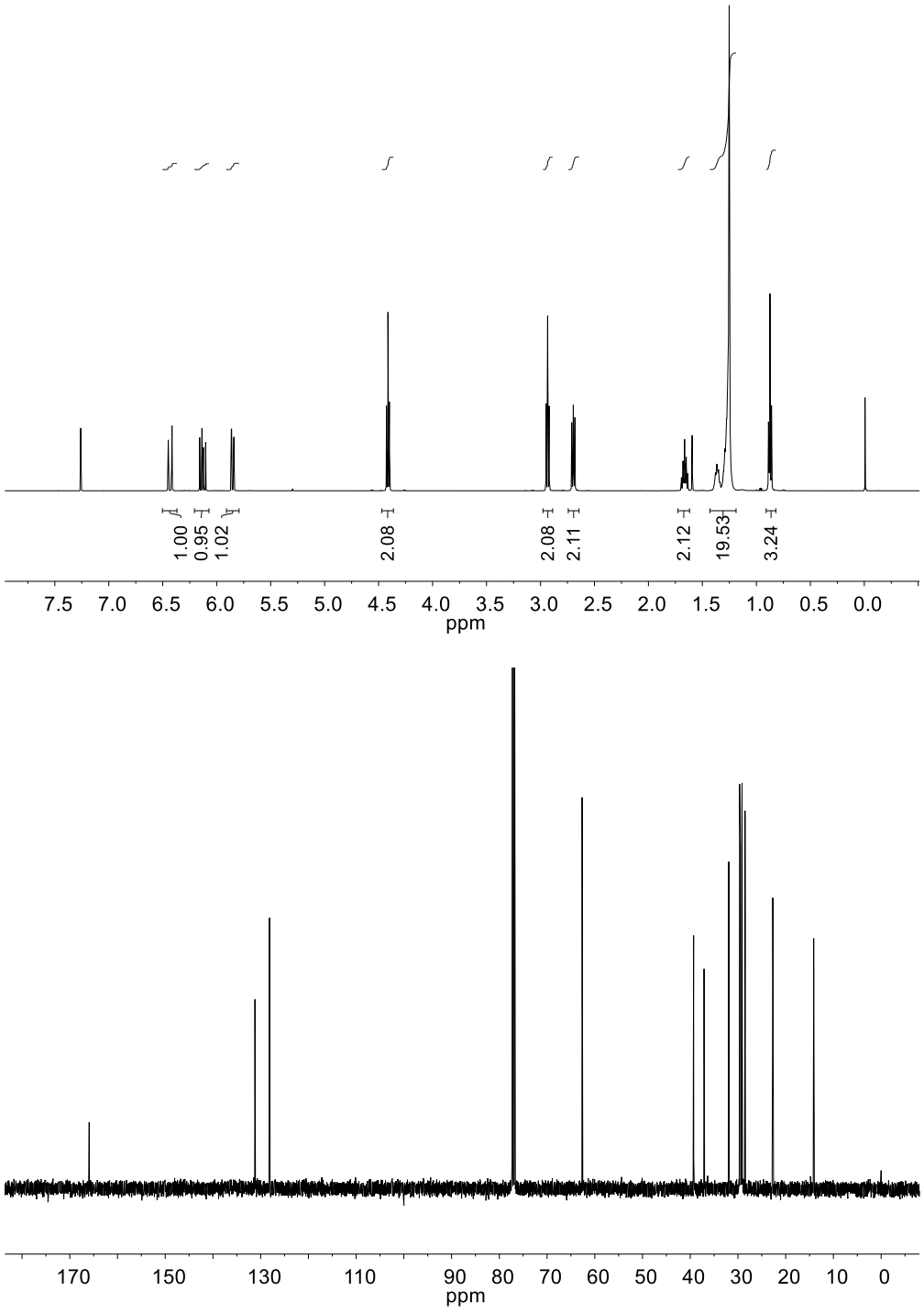

Figure 4. *^{1}H and ^{13}C NMR Spectra of O16B Lipidoids in $CDCl_3$.* ***(Top)*** *^{1}H NMR Spectra of O16B.* ***(Bottom)*** *^{13}C NMR Spectra of O16B.*

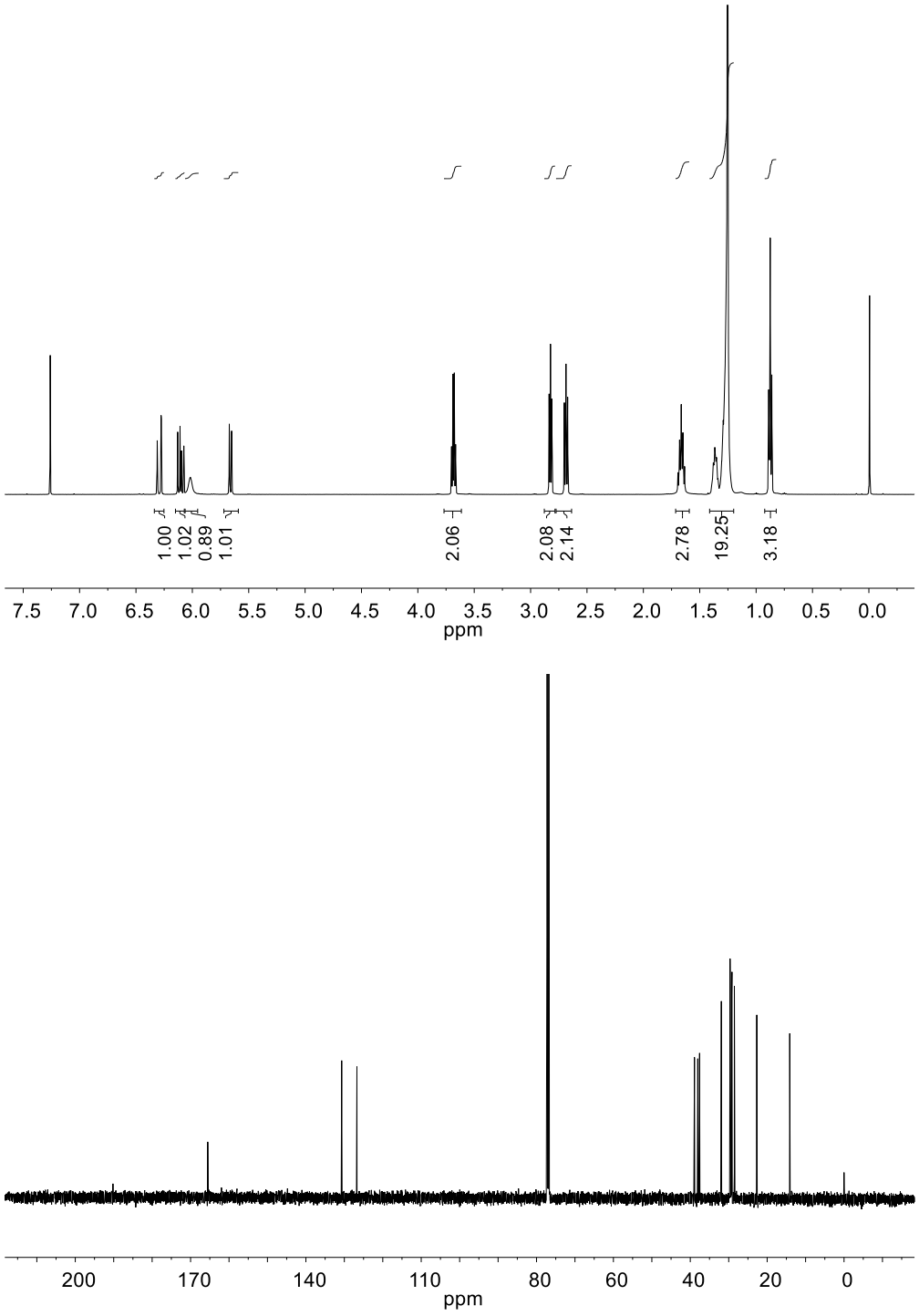

Figure 5. *^{1}H and ^{13}C NMR Spectra of N16B Lipidoids in $CDCl_3$.* ***(Top)*** *^{1}H NMR Spectra of N16B.* ***(Bottom)*** *^{13}C NMR Spectra of N16B.*

5.2. LNP Fabrication and Characterization

5.2.1. Fabrication

Formulated LNPs (Cas9:sgRNA/LNP) were formulated as outlined in Figure 15, while non-formulated LNPs (blank LNP) were initially prepared the same way, but no cholesterol/DOPE/PEG step was carried out, and the pure lipidoid products (80-O16B, e.g.) were dispersed as is in PBS. This yielded 40 unique LNP combinations (10 amine heads x 2 types of hydrophobic tail x 2 self-assembly methods) for testing purposes.

To begin the self-assembly fabrication of a LNP, aliquots of pure lipidoid, cholesterol, DOPE, and DSPE-PEG(2000) were prepared in solvents of chloroform at concentrations of 10 mg/mL. These lipidoid, cholesterol, DOPE, and DSPE-PEG(2000) solutions were combined in a clean glass vial at a 16:4:1:1 volumetric ratio to obtain 1 mg of pure lipid in the vial. This vial was stored uncovered at room temperature in a fume hood overnight (for at least 18 h), evaporating off the chloroform and leaving a solid film of material at the bottom of the vial. 100 µL of ethanol (100%) was added to this vial, enough to cover the film at the bottom of the vial completely, and the vial was capped and sonicated for 5-10 min to completely dissolve all materials. Separately, 800 µL of sodium acetate buffer (in nuclease-free water solution, 25 Mm, pH 5) was added to a

clean glass vial and stirred at a moderate speed using a small magnetic stir bar and stir plate. The contents of the lipidoid-in-ethanol vial was then added dropwise to the sodium acetate vial and stirred for 10 min. Finally, the contents of the stirring vial were added to a dialysis cassette using a sterile syringe. This filled cassette was subjected to dialysis by placing it into a clean 2 L glass beaker containing a stir bar and ~1.8 L of deionized water as the external buffer solution. The contents of the beaker were stirred at room temperature for at least 2 h, changing the solution after the first hour. The sample was extracted from the cassette at the end of the dialysis using a sterile syringe and transferred to a new glass vial, where it was labeled and stored at 4 degC for future use. The preparation of this LNP was carried out to achieve a target concentration of 1 mg/mL.

This process was carried out a total of 20 times to make one fabricated LNP sample of each lipidoid listed in Table 1.

5.2.2. Sample Preparation for Characterization

Samples of blank and RNP-loaded LNPs to be run through DLS and TEM equipment were prepared. A blank LNP is a lipid nanoparticle dispersed in PBS and not combined with any proteins, RNP or otherwise.

To prepare the blank LNP samples, the fabricated LNPs (1 mg/mL) were removed from refrigeration and combined with PBS in centrifuge tubes at a 1:50 volumetric ratio. These vials were left undisturbed for 30 min to again ensure thorough dispersion of materials. Finally, 120 µL of each vial was transferred to a

clean, deep-well square vial suitable for direct sample testing on DLS equipment. The target concentration of each LNP in each vial was 19.6 µg/mL.

To prepare the RNP-loaded LNP samples, an aliquot combining PBS, Cas9 protein (100 µM), and sgRNA (100 µM) was mixed in a 2000:3:3 volumetric ratio. This aliquot was mixed via pipette and left undisturbed for 20 min to ensure allow the materials to form a complex. The Cas9:sgRNA/PBS mixture was then transferred to different centrifuge tubes. The fabricated LNPs (1 mg/mL) were removed from refrigeration and combined with the Cas9:sgRNA/PBS mixtures in the centrifuge tubes at a 1:50 volumetric ratio. These vials were left undisturbed for 30 min to again ensure thorough complexing of materials. Finally, 120 µL of each vial was transferred to a clean, deep-well square vial suitable for direct sample testing on DLS equipment. The target concentration of each LNP in each vial was 19.6 µg/mL.

These samples were imaged with TEM equipment to confirm their structure. The samples were also tested through DLS equipment immediately upon their completion and once every 8 h over the course of 48 h. Hydrodynamic diameter ($<D_h>$) and polydispersity index (μ_2) values were obtained. Between tests, the samples were stored at 4 degC.

5.2.3. Physical Characterization

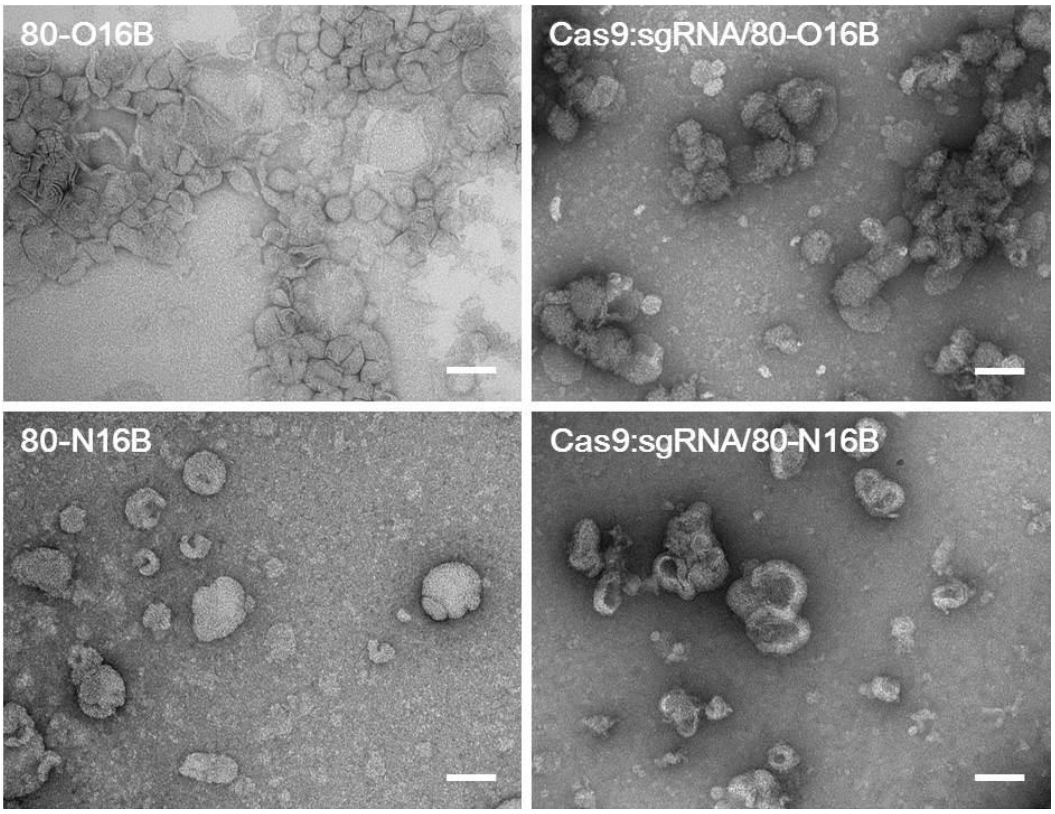

Figure 6. *Characterization of Blank and RNP-loaded LNPs Using TEM. Bar scale is 100 nm.*

Morphologies of the some LNPs were examined via TEM imaging. Figure 6 shows images of the blank 80-O16B, Cas9;sgRNA/80-O16B, Cas9:sgRNA/80-N16B, and blank 80-N16B (clockwise from top left) LNPs. The TEM images show mostly spherical and elliptical particles that appear to be between 80 and 200 nm in size, which is smaller than the values reported for the 80-O16B LNPs and smaller yet comparable to the values reported for the 80-N16B LNPs in Figure 7.

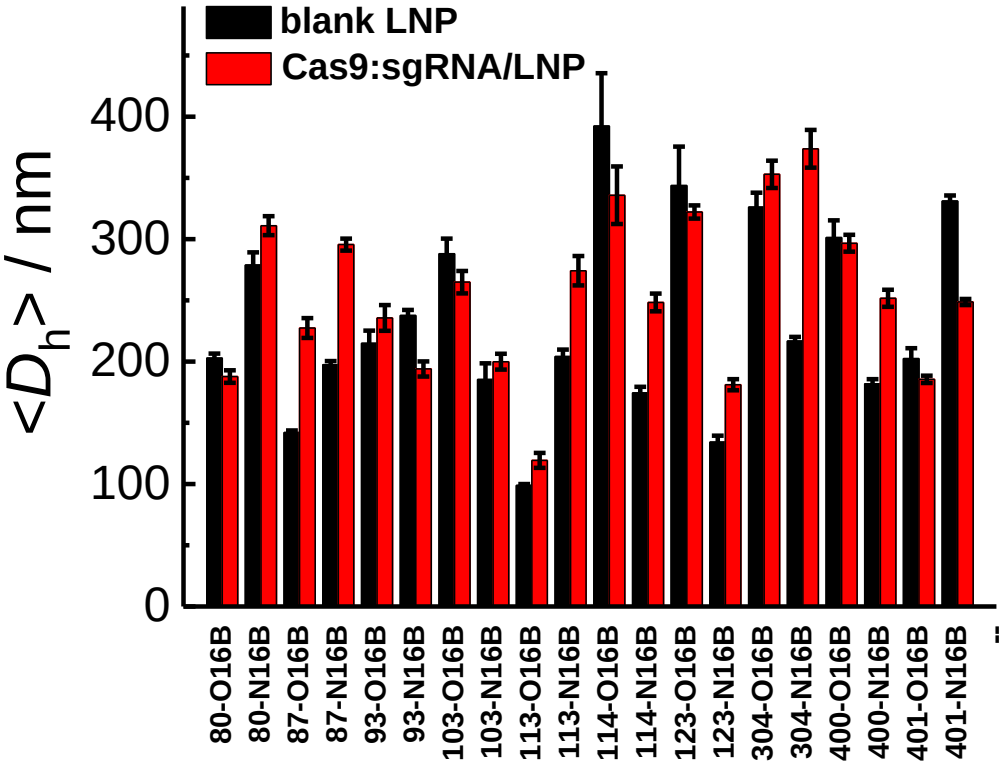

Figure 7. *Characterization of Blank and RNP-loaded LNPs Using DLS. Error bars are s.d.*

Samples of all 40 LNPs were subjected to DLS analysis to measure hydrodynamic diameter and polydispersity indexes every 8 h over the span of 48 h. Figure 7 shows the 0 h data from these tests. A clear majority of the 40 LNPs tested have average $<D_h>$ values between 100 and 350 nm. Breaking down the data further, ~2.5% of tested LNPs had $<D_h>$ values between 0 and 100 nm, ~27.5% had $<D_h>$ values between 100 and 200 nm, ~45% had $<D_h>$ values between 200 and 300 nm, and ~25% had $<D_h>$ values between 300 and 400 nm. These findings are similar to the values found in previously reported LNP data

from our lab and are anticipated to be well suited for applications involving intracellular protein delivery [3][19]. Across all LNP versions, 40% of blank LNPs had larger $<D_h>$ values than their Cas9:sgRNA/LNP analogues. Comparing O16B-tailed LNPs to their N16B-tailed analogues, 50% of blank O16B-tailed LNPs had larger $<D_h>$ values than their blank N16B-tailed LNPs analogues, while the amount of blank O16B-tailed LNPs which had larger $<D_h>$ values than their blank N16B-tailed LNPs analogues was also 50%.

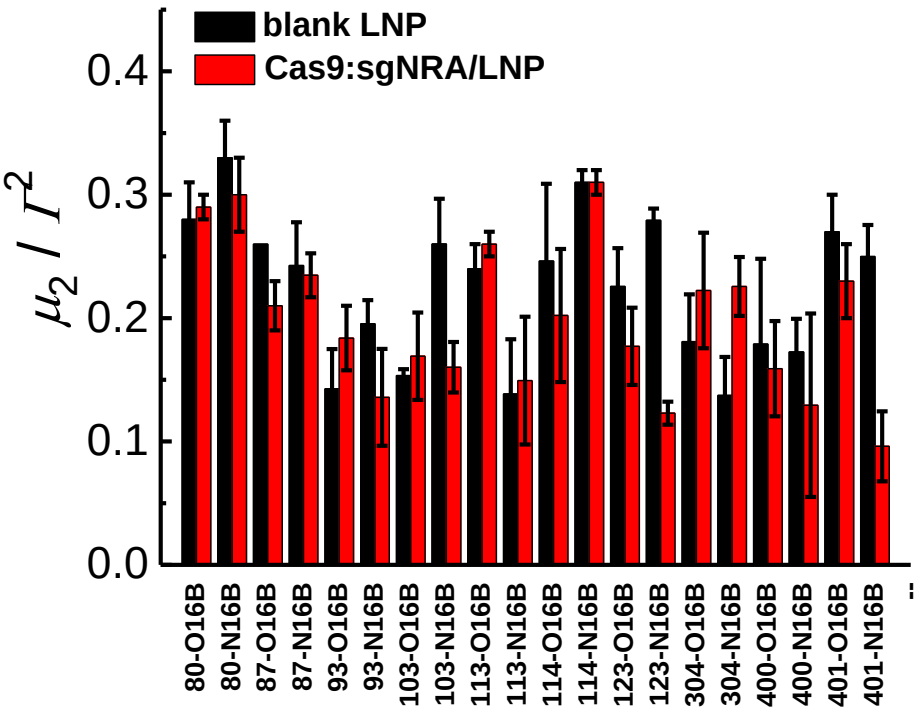

Figure 8. *Polydispersity Values of Blank and RNP-loaded LNPs Using DLS Measurements. Error bars are s.d.*

DLS analysis also showed that the polydispersity indices, a measurement of the distribution of molecular mass in a sample, of nearly all LNPs was between 0.1 and 0.3. These numbers, seen in Figure 8, further point to the uniformity and relative homogeneity of initial particle size as well as to a lack of aggregation of the LNPs.

5.2.4. Stability Tests

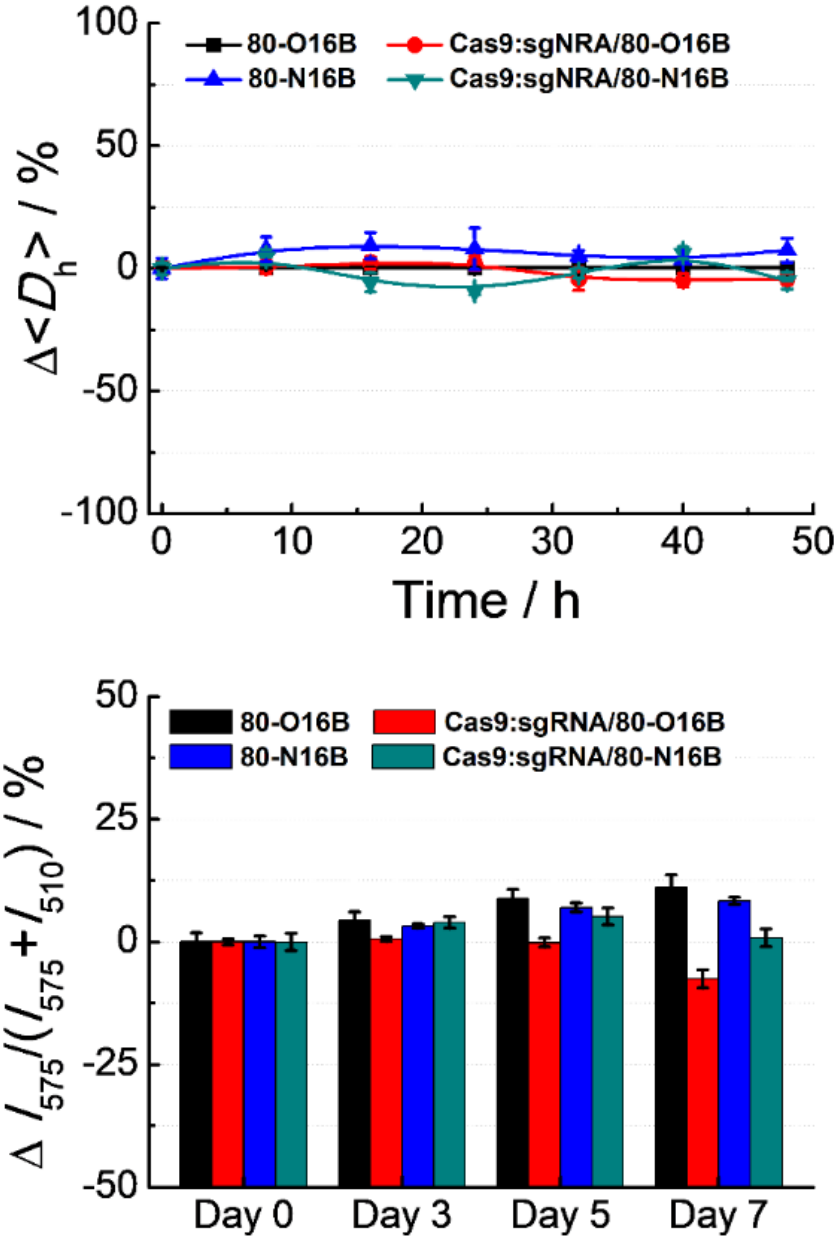

Figure 9. *Representative Stability Tests Using DLS and Fluorescence Spectrometer Measurements. Error bars are s.d.* ***(Top)*** *48 h Change in Mean Hydrodynamic Diameter for Representative LNP Sample, Blank and RNP-loaded.* ***(Bottom)*** *7 d Change in FRET Ratio Intensity for Representative LNP Sample, Blank and RNP-loaded.*

Figure 9a shows a representative example of the $<D_h>$ value variation exhibited by all LNP formulations over 48 h. Most LNP formulations exhibit a change in $<D_h>$ value of no greater than 25% at any of the 8 h intervals over the span of the study, indicating high stability with statistically insignificant aggregation over two days at room temperature for those formulations.

Images were also taken using a fluorescence spectrometer to check the structural integrity and overall stability of the LNPs. Blank and Cas9:sgRNA/LNPs of both 80-O16B and 80-N16B types show potential for extended storage, as Figure 9b showed fluorescence resonance energy transfer (FRET) ratio ($I_{575}/(I_{575}+I_{510})$) fluctuations of no greater than ~8% after 3 days and no greater than ~12.5% after 7 days.

The aggregate results of the 48 h stability study for O16B- and N16B-tailed Cas9:sgRNA/LNPs are given in Figure 10.

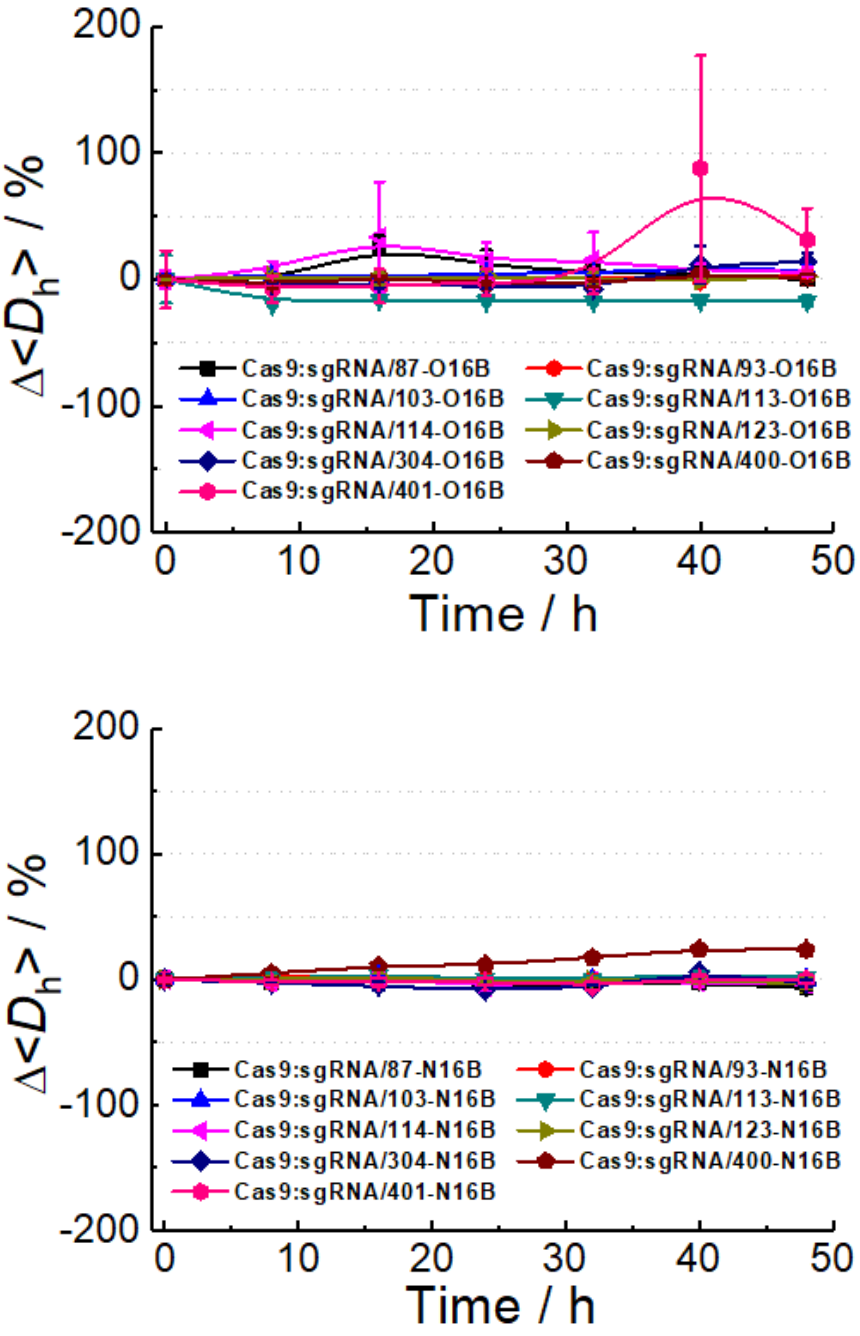

Figure 10. *Stability Test Using DLS Measurements. Error bars are s.d.* ***(Top)*** *48 h Change in Weighted Mean Hydrodynamic Diameter for O16B-tailed Cas9:sgRNA/LNPs.* ***(Bottom)*** *48 h Change in Mean Hydrodynamic Diameter for N16B-tailed Cas9:sgRNA/LNPs.*

5.3. Intracellular Delivery of GFP-Cre Using LNPs *In Vitro*

The first intracellular delivery study was conducted using green fluorescent protein fused to Cre recombinase (GFP-Cre) to test the LNPs for their ability to enable protein uptake by HeLa-DsRed cells by assessing GFP fluorescence at the intracellular level; this study was similar to a study previously done by our lab [3].

5.3.1. Intracellular Delivery Procedure

A 48-well Falcon plate was seeded with HeLa-DsRed cells dispersed in 250 µL of cell culture media per well at an initial concentration of 15000 cells per well and incubated overnight for at least 18 h.

Separately, an aliquot combining PBS and GFP-Cre (4 mg/mL) was prepared at a 79:1 volumetric ratio. This aliquot was mixed via pipette and left undisturbed for 20 min to ensure even dispersion. The GFP-Cre/PBS mixture was then transferred to different wells of a 96-well Falcon plate. The fabricated LNPs (1 mg/mL) were removed from refrigeration and combined with the GFP-Cre/PBS mixtures in the 96-well plate at a 1:9 volumetric ratio. This 96-well plate was left undisturbed for 30 min to ensure thorough complexing of materials. Finally, the GFP-Cre/LNP complexes were delivered to their designated wells in the 48-well plate at 10 µL per well and 2 wells per LNP. For this study, Lpf2k

was used as a positive control. The complexed proteins without LNP and PBS were used as negative controls. The target concentration of each LNP in each well was 3.85 µg/mL. The cells were immediately put into the incubator and left undisturbed for 48 h.

At the end of this 48 h incubation period, the 48-well plate was removed from the incubator and all media was removed. 70 µL of trypsin was added to each well, and the plate was again incubated for 5-7 min to detach the HeLa-DsRed cells from the bottom of the wells. During this incubation step, an aliquot of combining PBS and cell culture media was prepared at a 1:1 ratio. The plate was removed from the incubator and 230 µL of the PBS/cell culture media mixture was added to each well to neutralize the trypsin and further suspend the cells. The contents of each well were then transferred into clean plastic test tubes designated for use with the FACS equipment.

The samples were run through FACS equipment to count the cells and measure the number of GFP-positive cells to determine how the cellular uptake for the GFP-Cre/LNP complex differs across the various LNPs. Data was collected using BD CellQuest^{TM} Pro software. Preset instrument settings specific to the expected measurements for HeLa-DsRed cells were used when running this software. The resulting data files were analyzed using FlowJo® software.

For the purposes of this experiment, LNPs yielding higher percentages of GFP-positive cells are considered more effective, and therefore more desirable, at facilitating protein uptake by the cells.

5.3.2. Internalization Results

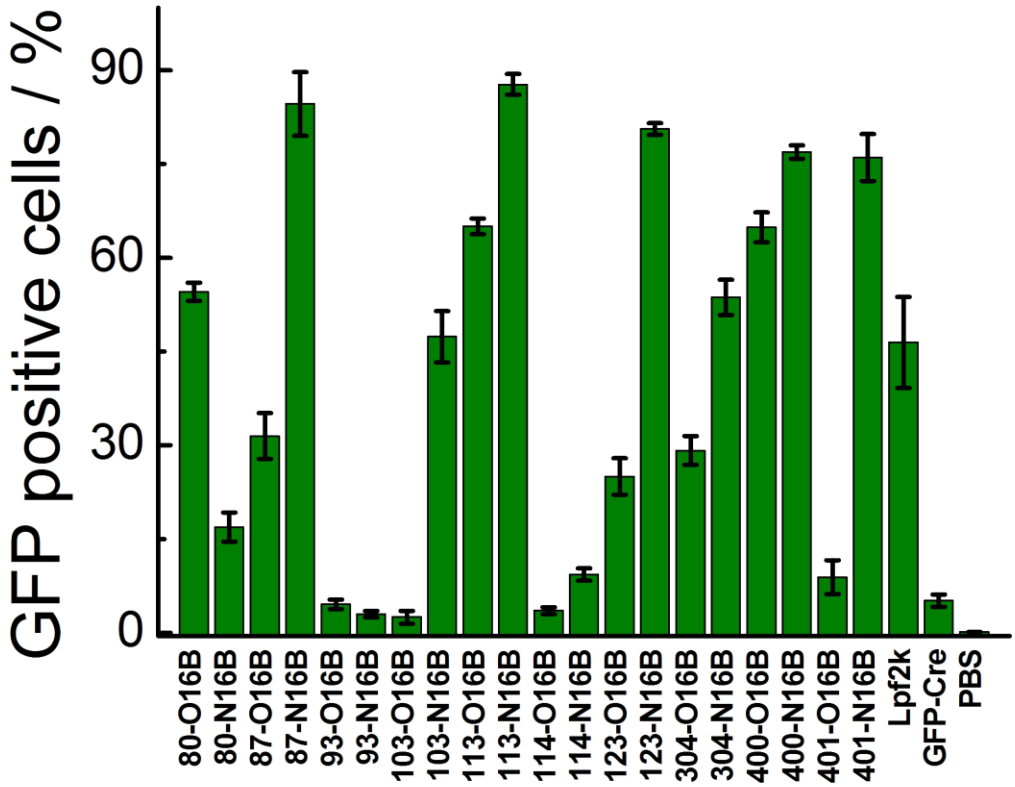

Figure 11. *Intracellular Delivery of GFP-Cre/LNP Complexes to HeLa-DsRed Cells for Efficacy of GFP-Cre Internalization. Error bars are s.d.*

One of our hypotheses was that GFP-Cre alone would not be able to enter cells. Figure 11 shows that this is mostly true, as GFP-Cre induced GFP-positive cells in only a percentage of cells only slightly higher (but still <15%) than the other negative control, PBS. The percent of LNPs that performed at a similar level to these negative controls was ~30%. LNPs such as 93-O16B and 103-O16B facilitated little to no GFP-positive cells. Another of our hypotheses was that

some of the LNPs would be able to facilitate the internalization of GF-Cre and induce GFP-positive cells at a similar efficacy to Lpf2k. As seen in Figure 11, ~55% of the LNPs tested performed better than or at a statistically similar level (>~45%) to the positive control, Lpf2k, with calculated errors considered. LNPs with the best performance were 87-N16B and 113-N16B, as these nanoparticles were able to readily facilitate the efficient uptake of GFP-Cre by the HeLa-DsRed cells, as shown by these LNPs inducing GFP-positive cells ~85% of the time. 123-N16B, 400-N16B, and 401-N16B also performed well, with ~82%, ~78%, and ~78% of the cells being identified as GFP-positive, respectively. Of the 10 pairs of amine heads compared, only 1 GFP-Cre/LNP delivery yielded little to no GFP-positive cells in either the O16B- or N16B-tailed case. Of the remaining 9 pairs, the N16B-tailed GFP-Cre/LNPs showed high efficacies of GFP-Cre internalization, and thereby resulting in more GFP-positive cells, to a statistically relevant degree ~89% of the time, while O16B-tailed Cas9:sgRNA/LNPs showed GFP-Cre internalization efficacy ~11% of the time. This may indicate that N16B-tailed LNPs generally perform better than the O16B-tailed LNPs at internalizing GFP-Cre into HeLa-DsRed cells, a theory which may carry over to other cell types and may be taken into consideration when formulating new LNPs for protein delivery based therapies.

5.4. Intracellular Delivery of Cas9:sgRNA Using LNPs *In Vitro*

The second intracellular delivery study was conducted using a Cas9:sgRNA complex (with the sgRNA specifically targeting GFP) to test the LNPs for their ability to deliver this complex to GFP-HEK cells by assessing their knockout efficacies.

5.4.1. Intracellular Delivery Procedure

A 48-well Falcon plate was seeded with GFP-HEK cells dispersed in 250 µL of cell culture media per well at an initial concentration of 15000 cells per well and incubated overnight for at least 18 h.

Separately, an aliquot combining PBS, Cas9 protein (100 µM), and sgRNA (100 µM) was mixed in a 2000:3:3 volumetric ratio. This aliquot was mixed via pipette and left undisturbed for 20 min to ensure allow the materials to form a complex. The Cas9:sgRNA/PBS mixture was then transferred to different wells of a 96-well Falcon plate. The fabricated LNPs (1 mg/mL) were removed from refrigeration and combined with the Cas9:sgRNA/PBS mixtures in the 96-well plate at a 1:9 volumetric ratio. This 96-well plate was left undisturbed for 30 min to again ensure thorough complexing of materials. Finally, the Cas9:sgRNA/LNP complexes were delivered to their designated wells in the 48-well plate at 10 µL per well and 2 wells per LNP. For this study, Lpf2k was used as a positive control. The complexed proteins without LNP and PBS were used as

negative controls. The target concentration of each LNP in each well was 3.85 µg/mL. The cells were immediately put into the incubator and left undisturbed for 48 h.

At the end of this 48 h incubation period, the 48-well plate was removed from the incubator and all media was removed. 70 µL of trypsin was added to each well, and the plate was again incubated for 5-7 min to detach the GFP-HEK cells from the bottom of the wells. During this incubation step, an aliquot of combining PBS and cell culture media was prepared at a 1:1 ratio. The plate was removed from the incubator and 230 µL of the PBS/cell culture media mixture was added to each well to neutralize the trypsin and further suspend the cells. The contents of each well were then transferred into clean plastic test tubes designated for use with the FACS equipment.

The samples were run through FACS equipment to measure their rate of GFP knockout by counting the number of GFP-negative cells to assess how the Cas9:sgRNA/LNP complexes are able to transfect the GFP-HEK cells across the various LNPs. Data was collected using BD CellQuest™ Pro software. Preset instrument settings specific to the expected measurements for GFP-HEK cells were used when running this software. The resulting data files were analyzed using FlowJo® software.

For the purposes of this experiment, LNPs yielding higher percentages of GFP negative cells are considered more effective, and therefore more desirable, at transfecting and altering GFP-HEK cells.

5.4.2. Internalization Results

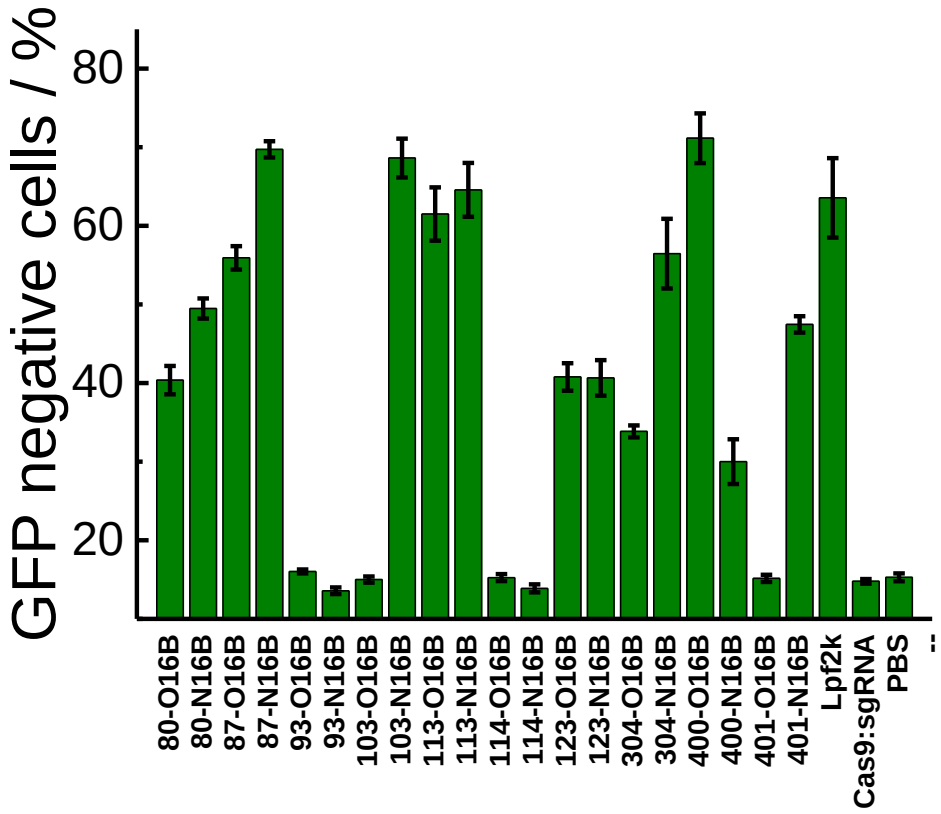

Figure 12. *Intracellular Delivery of Cas9-sgRNA/LNP Complexes to GFP-HEK Cells for GFP Gene Knockout. Error bars are s.d.*

One of our hypotheses was that the Cas9:sgRNA complex alone would not be able to enter the cells. Figure 12 shows that this is indeed the case, as Cas9:sgRNA induced the same level of GFP knockout (i.e. minimal) as the other negative control, PBS. The percent of LNPs which performed at a similar level to these negative controls was ~30%. LNPs such as 93-N16B and 114-N16B exhibited little to no transfection into the GFP-HEK cells. Another of our hypotheses was that some of the LNPs would be able to transfect the cells at an

efficiency comparable to Lpf2k. As seen in Figure 12, ~30% of the LNPs tested performed better than or at a statistically similar level (>~65%) to the positive control, Lpf2k, with calculated errors considered. LNPs with the best performance were 87-N16B, 103-N16B, and 400-O16B, as these nanoparticles were able to transfect the GFP-HEK cells and knockout GFP ~70% of the time. 113-O16B and 113-N16B also performed well, showing ~62% and ~65% knockout rates, respectively. Of the 10 pairs of amine heads compared, 2 showed little to no GFP knockout in either the O16B- or N16B-tailed Cas9:sgRNA/LNPs. Of the remaining 8 pairs, the N16B-tailed Cas9:sgRNA/LNPs showed greater GFP knockout efficiency to a statistically relevant degree ~62.5% of the time, while O16B-tailed Cas9:sgRNA/LNPs showed better knockout efficiency ~12.5% of the time. This may indicate that N16B-tailed LNPs generally perform better than the O16B-tailed LNPs at delivering Cas9:sgRNA to GFP-HEK cells. Future research could assess more commercially available amine heads with combinations of O16B- and N16B-based tails across other cell types to further verify or broaden this hypothesis. Figure 12 illustrates that many of the LNPs produced for this study were effective at knocking out GFP in GFP-HEK cells, indicating that these LNPs could prove valuable in further studies surrounding the delivery of intracellular proteins.

5.5. Measurement of Cytotoxicity *In Vitro*

The cytotoxicity of the formulated and unformulated LNPS in GFP-HEK cells were measured via MTT assay following previously outlined protocols [20][21]. As an additional experiment, a hemolysis assay was carried out in accordance with previously published methods [22].

5.5.1. MTT Assay Procedure

A 96-well plate was seeded with GFP-HEK cells at an initial concentration of 5000 cells per well dispersed in 100 µL of DMEM media per well and incubated overnight for at least 18 h. A cas9:sgRNA/LNP solution was prepared for each LNP as previously mentioned and added to the plate (4 µL per well, 4 wells per LNP). The Cas9:sgRNA/LNP complexes were delivered to their designated wells in the 96-well plate at 4 µL per well and 4 wells per LNP. For this study, Lpf2k was used as a positive control. The complexed proteins without LNP and PBS were used as negative controls. The target concentration of each LNP in each well was 3.85 µg/mL. The cells were immediately put into the incubator and left undisturbed for 48 h.

To complete the assay, a separate solution of MTT reagent was made by dispersing MTT into PBS buffer at a ratio of 5 mg per mL and sonicated for 5-10 min to completely dissolve all materials.

At the end of this 48 h incubation period, the 96-well plate was removed from the incubator and all media was removed. 30 µL of this MTT reagent was added to each well, and the cells were again incubated for 2 h. At the end of this 2 h incubation period, the 96-well plate was removed from the incubator and 200 µL dimethyl sulfoxide (DMSO) was added to each well. The plate was gently agitated by an orbital shaker for 10 min.

Absorbance measurements were immediately read by a microplate reader at a wavelength of 570 nm. The calculation $A_{LNP,570}$ / $A_{ctrl,570}$ x 100% was used to determine the viability of the GFP-HEK cells, where $A_{LNP,570}$ and $A_{ctrl,570}$ are the absorbances of wells treated with LNPs or a positive/negative control and the absorbances of untreated wells, respectively, at 570 nm.

5.5.2. MTT Results

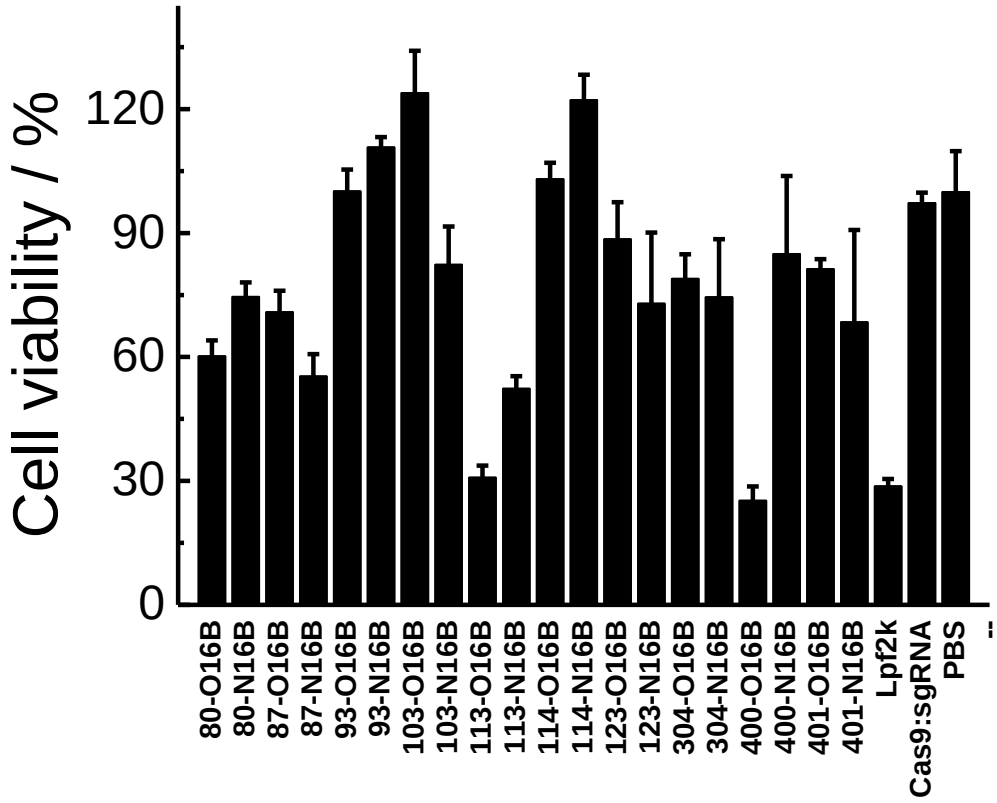

Figure 13. *Cytotoxicity Results from MTT Assay of Cas9:sgRNA/LNPs Delivered to GFP-HEK Cells. Error bars are s.d.*

Figure 13 shows that, of the LNPs tested, ~25% exhibited high cytotoxicity (cell viability <60%), with 113-O16B (~30% cell viability) and 400-O16B (<30%) performing the most comparably to Lpf2k, which was also highly cytotoxic (~30%). Notably, ~30% of the LNPs exhibited very low cytotoxicity (cell viability >~90%), with 93-N16B (~110%), 103-O16B (~120%), and 114-N16B (~120%) having the most favorable performance with respect to cells

staying alive after LNP treatment. This indicates that many of the tested LNPs have cytotoxicities low enough to be considered potentially viable for protein delivering therapeutics.

5.5.3. Hemolysis Assay

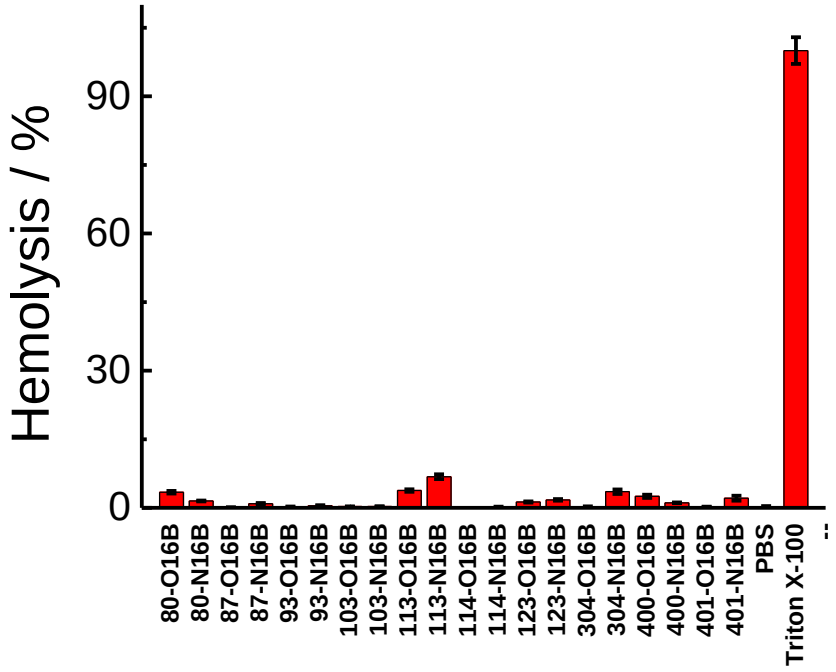

Figure 14. *Hemolysis Analysis of LNPs. Error bars are s.d.*

A hemolysis test was also performed to determine if the LNPs caused rupturing of red blood cells, using Triton X-100 and PBS as controls. Figure 14 shows that while LNPs like 113-O16B and 113-N16B appeared to induce a minimal amount of hemolysis, the majority of LNPs tested were shown to induce a negligible amount of hemolysis.

6. Discussion of LNP Performance

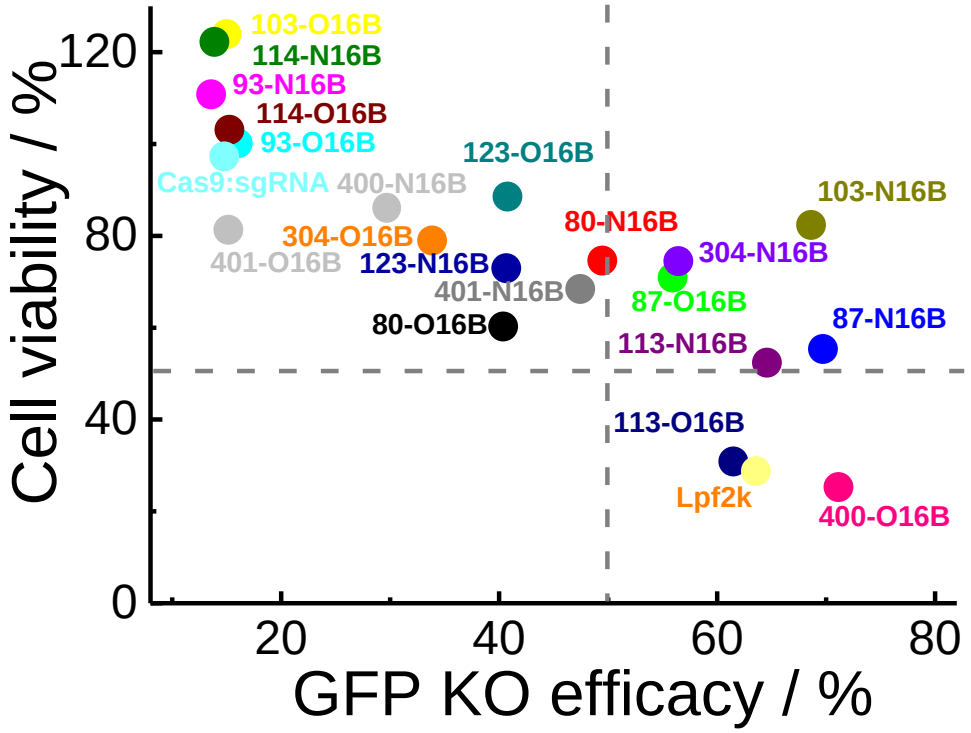

Figure 15. *Cell Viability Based on MTT Assay Against GFP Knockout Efficacy.*

Two important factors for determining which LNPs might be best suited for future protein-based therapies involving intracellular delivery are their abilities to transfect cells to affect desired changes and to not kill the cells into which they have been transfected. Figure 15 plots cell viability (from Figure 13) against GFP knockout efficacy (from Figure 12), with dotted lines denoting 50% values for both categories to create four quadrants. In general, it is obvious from Figure 15 that cell viability is negatively correlated with GFP knockout efficacy, which could potentially be expected because every cell that is transfected has the

LNP as a newly introduced foreign entity that could interfere with the homeostasis of the cell. It is also interesting to note that congeners differing by merely one atom (O vs N) can have very different viability/transfection profiles.

Of the 20 unique Cas9:sgRNA/LNPs tested in this study, 0% had poor cell viability and poor GFP knockout efficacy (lower left quadrant). A 65% majority of LNPs had high cell viability and poor GFP knockout efficacy (upper left quadrant), meaning these LNPs did less to harm the cells than some of their counterparts, but also did not deliver the Cas9:sgRNA complex to the target effectively. The Cas9:sgRNA complexed without LNP was found in this region. Another 10% of the LNPs had low cell viability and high GFP knockout efficacy (lower right quadrant), meaning these LNPs delivered the complex to the cells effectively while also destroying many of these cells in the process. The Lpf2k was found in this region.

By far the most promising group of LNPs are those with high cell viability and high GFP knockout efficacy (upper right quadrant), a subpopulation which comprised 25% of the LNPs tested. Of the 5 LNPs in this quadrant, 4 were N series LNPs.

Detailing this region further, 87-O16B (~70% cell viability, ~55% GFP KO efficacy) and 304-N16B (~75%, ~56%) were LNPs with high cell viability and adequate knockout efficacy, while 113-N16B (~53%, ~64%) and 87-N16B (~55%, ~69%) had adequate cell viability and high knockout efficacy. The best performing LNP, however, was 103-N16B (~83%, ~68%), exhibiting a combination of both high cell viability and knockout efficacy. This LNP along

with any of the lipid nanoparticles found in the upper right quadrant of Figure 15 are strong candidates for future studies surrounding the delivery of protein-based therapies.

7. Conclusions and Future Impact

To summarize, we fabricated 20 unique lipid nanoparticles by combining a new library of synthesized lipid products with cholesterol, DOPE, and C16-PEG-DSPE to create 10 pairs of formulated LNPs, with each congener pair differing by only one atom. To begin the analysis, the LNPs were assessed for structure, morphology, stability, hydrodynamic diameter, and polydispersity using 1H and 13C NMR spectra, TEM, DLS, and FRET testing. These results show that, in general, the LNPs were stable over the short- and long-term with consistent, expected sizes and appearances. The LNPs were complexed with GFP-Cre and delivered to HeLa-DsRed cells to test internalization efficacy of GFP-Cre. We report that many of the LNPs tested were able to induce GFP-positive cells at a rate equal to or greater than an effective, commercially available positive control. The LNPs were also complexed with cas9:sgRNA to target and knockout the GFP gene and resulting fluorescence found in GFP-HEK cells. We report that many of the LNPS tested were able to knockout GFP at a rate equal to or greater than that of the positive control. Differences between GFP-Cre internalization and GFP knockout efficacies caused by different congeners of LNPs were identified, with a subset of the formulated LNPs showing a clear advantage when considering future experiments. Assays were carried out to determine the toxicity of the LNPs to GFP-HEK and red blood cells, showing that many of the LNPs did not induce cell death to statistically detrimental degree in these treatments. The sum results of these findings were analyzed and a plot of cell viability against

GFP knockout efficacy was creating and detailed, illustrating how changing one atom in the tail of a LNP can produce varying results with respect to intracellular delivery and yielding a group of strong candidates for further research into using lipidoid structures to deliver protein-based therapies.

8. References

[1] Fu, A., Tang, R., Hardie, J., Farkas, M. E., & Rotello, V. M. (2014). Promises and pitfalls of intracellular delivery of proteins. Bioconjugate chemistry, 25(9), 1602-1608.

[2] Bhatia, S. (2016). Natural Polymer Drug Delivery Systems: Nanoparticles, Plants, and Algae. Springer.

[3] Wang, M., Zuris, J. A., Meng, F., Rees, H., Sun, S., Deng, P., ... & Georgakoudi, I. (2016). Efficient delivery of genome-editing proteins using bioreducible lipid nanoparticles. Proceedings of the National Academy of Sciences, 113(11), 2868-2873.

[4] Quianzon, C. C., & Cheikh, I. History of insulin. J Community Hosp Intern Med Perspect 2012; 2.

[5] Dimitrov, D. S. (2012). Therapeutic proteins. In Therapeutic Proteins (pp. 1-26). Humana Press, Totowa, NJ.

[6] Leader, B., Baca, Q. J., & Golan, D. E. (2008). Protein therapeutics: a summary and pharmacological classification. Nature reviews Drug discovery, 7(1), 21.

[7] Kong, L., Zhang, X., Li, C., & Zhou, L. (2017). Potential therapeutic targets and small molecular drugs for pediatric B-precursor acute lymphoblastic leukemia treatment based on microarray data. Oncology letters, 14(2), 1543-1549.

[8] Torres, T., & Filipe, P. (2015). Small molecules in the treatment of psoriasis. Drug development research, 76(5), 215-227.

[9] Reichert, J. M. (2003). A guide to drug discovery: Trends in development and approval times for new therapeutics in the United States. Nature Reviews Drug Discovery, 2(9), 695.

[10] Barrangou, R. (2015). The roles of CRISPR–Cas systems in adaptive immunity and beyond. Current opinion in immunology, 32, 36-41.

[11] Doudna, J. A., & Charpentier, E. (2014). The new frontier of genome engineering with CRISPR-Cas9. Science, 346(6213), 1258096.

[12] Liu, C., Zhang, L., Liu, H., & Cheng, K. (2017). Delivery strategies of the CRISPR-Cas9 gene-editing system for therapeutic applications. Journal of Controlled Release.

[13] Shah, R., Eldridge, D., Palombo, E., & Harding, I. (2015). Lipid nanoparticles: Production, characterization and stability (pp. 11-22). New York: Springer International Publishing.

[14] Tabatt, K., Kneuer, C., Sameti, M., Olbrich, C., Müller, R. H., Lehr, C. M., & Bakowsky, U. (2004). Transfection with different colloidal systems: comparison of solid lipid nanoparticles and liposomes. Journal of controlled release, 97(2), 321-332.

[15] Platt, R. J., Chen, S., Zhou, Y., Yim, M. J., Swiech, L., Kempton, H. R., ... & Graham, D. B. (2014). CRISPR-Cas9 knockin mice for genome editing and cancer modeling. Cell, 159(2), 440-455.

[16] Raghavan, A., Wang, X., Rogov, P., Wang, L., Zhang, X., Mikkelsen, T. S., & Musunuru, K. (2016). High-throughput screening and CRISPR-Cas9 modeling of causal lipid-associated expression quantitative trait locus variants. bioRxiv, 056820.

[17] Mali, P., Aach, J., Stranges, P. B., Esvelt, K. M., Moosburner, M., Kosuri, S., ... & Church, G. M. (2013). CAS9 transcriptional activators for target specificity screening and paired nickases for cooperative genome engineering. Nature biotechnology, 31(9), 833.

[18] Wang, M., Alberti, K., Sun, S., Arellano, C. L., & Xu, Q. (2014). Combinatorially Designed Lipid-like Nanoparticles for Intracellular Delivery of Cytotoxic Protein for Cancer Therapy. Angewandte Chemie, 126(11), 2937-2942.

[19] Sun, S., Wang, M., Knupp, S. A., Soto-Feliciano, Y., Hu, X., Kaplan, D. L., ... & Xu, Q. (2011). Combinatorial library of lipidoids for in vitro DNA delivery. Bioconjugate chemistry, 23(1), 135-140.

[20] Provost, J. & Wallert, M. (1998). MTT Proliferation Assay Protocol. Cell Based Assays & Protocols. Department of Chemistry and Biochemistry, University of San Diego. Web. 04 January 2018.

[21] Li, Y., Qian, Y., Liu, T., Zhang, G., & Liu, S. (2012). Light-triggered concomitant enhancement of magnetic resonance imaging contrast performance and drug release rate of functionalized amphiphilic diblock copolymer micelles. Biomacromolecules, 13(11), 3877-3886.

[22] Li, Y., Hu, X., Tian, S., Li, Y., Zhang, G., Zhang, G., & Liu, S. (2014). Polyion complex micellar nanoparticles for integrated fluorometric detection and bacteria inhibition in aqueous media. Biomaterials, 35(5), 1618-1626.